Accurate Iterative Reconstruction Algorithm for Sparse Objects: Application to 3-D Blood-Vessel Reconstruction from a Limited Number of Projections

Meihua Li[1], Haiquan Yang[2], and Hiroyuki Kudo[3]
[1]Doctoral Program in Engineering, University of Tsukuba, Tsukuba 305-8573, Japan
[2]Department of Mathematics, Jilin University, Changchun 130012, Jilin, China
[3]Institute of Information Sciences and Electronics, University of Tsukuba, Tsukuba 305-8573, Japan

Abstract

This paper proposes an accurate row-action type iterative method which is appropriate to reconstruct sparse objects from a limited number of projections. The main idea is to use the L_p norm with $p \approx 1.1$ to pick up a sparse solution from a set of feasible solutions to the measurement equation. We also show that this method works well in the 3-D blood-vessel reconstruction.

I. Introduction

Image reconstruction from a limited number of projections is a well-investigated subject in tomographic reconstruction fields. For example, this problem possesses applications in visualization of 3-D blood-vessel structure from angiographic projections and cardiac imaging with various modalities [1]. In spite of a lot of works, however, it is fair say that successful reconstruction algorithms which can be used in clinical routine do not exist. This paper proposes an iterative reconstruction algorithm which is very powerful for sparse objects. Here, the sparse objects refer to objects which have non-zero pixel values only on a relatively small number of pixels. Such objects appear in many instances of tomographic imaging. In particular, we have the following three applications in mind. The first application is the reconstruction of cerebral or cardiac blood-vessel structure from a limited number of angiographic projections measured with a C-Arm or rotational-angiographic devices (digital subtraction technique is normally used to eliminate unnecessary background objects). The second application is the cardiac SPECT or PET imaging where the cross section can be approximately regarded as a sparse object because the isotope normally concentrates only on the heart. The last interesting application is the reconstruction of tomographic dynamic sequences. This problem can be also formulated as the reconstruction of a sparse object in the following way. Let t denote time and assume that we have a good reconstruction f_t at time t. Then, $f_{t+1} - f_t$ becomes a sparse object if the motion in the cross section is not so large. Therefore, we can reconstruct $f_{t+1} - f_t$ from a limited number of projections g_{t+1} at time $t+1$ if an accurate reconstruction algorithm for sparse objects exists, which leads to an accurate reconstruction of f_{t+1}.

The proposed algorithm is outlined as follows. The tomographic reconstruction problem can be formulated as solving a linear equation $A\vec{x} = \vec{b}$ where $\vec{x}$ is an image vector, $\vec{b}$ is a set of measured line integrals, and A is an $m \times n$ matrix relating $\vec{x}$ to $\vec{b}$. When the number of projections is small, many feasible solutions to $A\vec{x} = \vec{b}$ exist because $m < n$. To pick up a good solution having sparsity from a set of feasible solutions, we formulate the problem as a bound-constrained minimum norm problem (PPB):

$$\text{minimize } \| \vec{x} \|_p^p /p \text{ subject to } A\vec{x} = \vec{b} \text{ and } 0 \leq \vec{x} \leq 1$$

where $\| \vec{x} \|_p$ denotes the L_p norm of $\vec{x}$ and the inequality $0 \leq \vec{x} \leq 1$ can be understood componentwise. The value of norm parameter p has a large effect on the solution. The best value of p for sparse objects is $p = 0$ because $\lim_{p \to 0} \| \vec{x} \|_p^p$ is equivalent to the number of non-zero pixels. This choice allows to pick up an object which has minimum number of non-zero pixels. However, $\| \vec{x} \|_p^p /p$ is non-convex and is non-differentiable when $0 < p < 1$ which makes it impossible to use well-known convex optimization techniques to construct an iterative algorithm. To overcome this drawback, we use $p \approx 1.1$ (a slightly larger value than 1). For this choice, $\| \vec{x} \|_p^p /p$ is both convex and differentiable so that we can use standard convex optimization techniques. Furthermore, $p \approx 1.1$ still allows to pick up a sparse solution to $A\vec{x} = \vec{b}$ compared to the use of ordinary Euclidean norm $p = 2$. We construct an iterative method for the above constrained minimization problem by using the dual coordinate ascent method [2]. This method converts the original problem (PPB) into a dual problem by using the so-called Lagrangian duality. Since the dual problem corresponding to (PPB) becomes a simple unconstrained maximization problem, we solve it by using the coordinate ascent method. In the primal space, this method can be considered as a variant of Bregman's method for convex programming excepting the bound constraint $0 \leq \vec{x} \leq 1$ [3]. The resulting algorithm is of row-action type similarly to the Algebraic Reconstruction Technique (ART). The iteration converges fast by using a projection access order proposed in the literature [4].

We believe that this method possesses some important applications in tomography. As a first step, we have applied this method to the reconstruction of 3-D blood-vessel structure from a limited number of cone-beam projections. The simulation results demonstrate that an accurate reconstruction is possible from only 8 projections for which the Feldkamp method and the ART method are not valid anymore. Furthermore, we apply the method to real-data measured with the cone-beam tomographic imaging system using a synchrotron radiation x-ray source [5].

II. Proposed Method

A. Problem Formulation

In tomography, the goal is to reconstruct an object from line-integral projection data. A discrete version of the projection process can be represented as

$$A\vec{x} = \vec{b}$$

where $A = (a_{ij})$ is a real $m \times n$ matrix representing the projection operator, $\vec{x} = (x_1, \cdots, x_n)^\top$ is a real vector representing the object, and $\vec{b} = (b_1, \cdots, b_m)^\top$ is the corresponding projection data. Let $\vec{c}_j$ denote the j-th column of matrix A.

For convenience to explain the method, we first consider the following minimum norm problem (PP):

$$\text{minimize } \| \vec{x} \|_p^p / p \text{ subject to } A\vec{x} = \vec{b} \tag{1}$$

where $1 < p < 2$. We use $p \approx 1.1$ for sparse objects as mentioned in Section I. Though the problem (PP) is simpler than the problem (PPB), it is still a nonlinear constrained optimization, and is difficult to solve directly. However, its dual will be an unconstrained optimization.

B. Lagrangian Duality

From the reference [6], the Lagrangian dual of the problem (PP) is the following maximization problem (DP):

$$\text{maximize } D(\vec{y}) = \vec{b}^\top \vec{y} - \| A^\top \vec{y} \|_q^q / q \tag{2}$$

where $\vec{y} = (y_1, \cdots, y_m)^\top$ is a real vector, and $q = p/(p-1)$. Let $\vec{z}(\vec{y}) = (z_1(\vec{y}), \cdots, z_n(\vec{y}))^\top$ be a vector function whose j-th component is $z_j(\vec{y}) = |\vec{c}_j^\top \vec{y}|^{q-1} \mathrm{sign}(\vec{c}_j^\top \vec{y})$. If $\vec{x}^*$ solves the problem (PP), then there exists $\vec{y}^*$ such that $\vec{x}^* = \vec{z}(\vec{y}^*)$ and $\vec{y}^*$ solves the problem (DP). Conversely, let $\vec{y}^*$ solve the problem (DP), then the vector $\vec{x}^* = \vec{z}(\vec{y}^*)$ solves the problem (PP).

C. Solving Maximization Problem (DP)

Obviously, the number of the unknowns in the problem (DP) is less than that in the problem (PP). Furthermore, the problem (DP) is an unconstrained maximization which is easier to solve than the problem (PP).

Differentiating (2), we get the following equations:

$$D'_{y_i}(\vec{y}) = 0, \quad i = 1, \cdots, m. \tag{3}$$

Equation (3) is a system of nonlinear equations which yields a solution of (2). Using the newton-like iteration to each equation in parallel, we get

$$y_i^{(k+1)} = y_i^{(k)} - \beta \frac{D'_{y_i}(\vec{y}^{(k)})}{D''_{y_i y_i}(\vec{y}^{(k)})}, \quad i = 1, \cdots, m. \tag{4}$$

where β is the relaxation parameter. We define

$$\Delta_i(\omega_1, \cdots, \omega_n) = \frac{b_i - \sum_{j=1}^{n} a_{ij} |\omega_j|^{q-1} \mathrm{sign}(\omega_j)}{(q-1) \sum_{j=1}^{n} (a_{ij})^2 |\omega_j|^{q-2}},$$

then for $i = 1, \cdots, m$, (4) can be written as

$$y_i^{(k+1)} = y_i^{(k)} + \beta \Delta_i(\vec{c}_1^\top \vec{y}^{(k)}, \cdots, \vec{c}_n^\top \vec{y}^{(k)}), \tag{4'}$$

In fact, for convenience to implement, we use the sequential Gauss-Seidel type iteration scheme (5) in our program:

$$y_i^{(k+1)} = y_i^{(k)} + \beta \Delta_i(\omega_1^{(k,i)}, \cdots, \omega_n^{(k,i)}), \quad i = 1, \cdots, m, \tag{5}$$

where $\omega_j^{(k,i)} = \sum_{l=1}^{i-1} a_{lj} y_l^{(k+1)} + \sum_{l=i}^{m} a_{lj} y_l^{(k)}$ is another expression of $\vec{c}_j^\top \vec{y}$ in the iteration. Equation (5) can be regarded as the coordinate ascent method applied to maximize $D(\vec{y})$.

D. Algorithm

According to the duality, if $\vec{x}^*$ and $\vec{y}^*$ are solutions of the problems (PP) and (DP) respectively, then $x_j^* = |\vec{c}_j^\top \vec{y}^*|^{q-1} \mathrm{sign}(\vec{c}_j^\top \vec{y}^*)$, $j = 1, \cdots, n$. Though it is difficult to get an explicit iteration scheme for $\vec{x}$, we can get one for $\omega_j^{(k,i)}$. We define $\vec{\mu}^{(k,i)} = (y_1^{(k+1)}, \cdots, y_{i-1}^{(k+1)}, y_i^{(k)}, y_{i+1}^{(k)}, \cdots, y_m^{(k)})^\top$, $\vec{\mu}^{(k,i+1)} = (y_1^{(k+1)}, \cdots, y_{i-1}^{(k+1)}, y_i^{(k+1)}, y_{i+1}^{(k)}, \cdots, y_m^{(k)})^\top$, $\vec{\mu}^{(k,m+1)} = \vec{\mu}^{(k+1,1)}$, $\omega_j^{(k,i)} = \vec{c}_j^\top \vec{\mu}^{(k,i)}$, and $\omega_j^{(k,m+1)} = \omega_j^{(k+1,1)}$. Let $\vec{\Omega}^{(k,i)} = (\overbrace{0, \cdots, 0}^{i-1}, \Delta_i(\omega_1^{(k,i)}, \cdots, \omega_n^{(k,i)}), \overbrace{0, \cdots, 0}^{m-i})^\top$. Then from (5), we obtain

$$\vec{\mu}^{(k,i+1)} = \vec{\mu}^{(k,i)} + \beta \vec{\Omega}^{(k,i)}. \tag{5'}$$

Taking an inner product with $\vec{c}_j$, we finally get

$$\omega_j^{(k,i+1)} = \omega_j^{(k,i)} + \beta a_{ij} \Delta_i(\omega_1^{(k,i)}, \cdots, \omega_n^{(k,i)}), \tag{6}$$

$$j = 1, \cdots, n.$$

Note that (6) is a row-action type iteration. Note also that (6) is exactly the ART method when $p = 2$. Unfortunately, the iteration is instable when the denominator of Δ_i in (6) is near 0. In our program, we set the denominator to a real constant MIN if its value is less than the constant MIN.

The algorithm is summarized as follows.

[STEP 1] Give an initial vector $\vec{\omega}^{(0)} = (\omega_1^{(0)}, \cdots, \omega_n^{(0)})^\top$ such that $\vec{\omega}^{(0)} = A^\top \vec{y}^{(0)}$ for some $\vec{y}^{(0)}$. ■

[STEP 2] For $k = 0, 1, \cdots$, do the following iteration until k is large enough or $\| \vec{\omega}^{(k)} - \vec{\omega}^{(k+1)} \|$ is small enough. ■

[STEP 2.1] Let $\vec{\omega}^{(k,1)} = \vec{\omega}^{(k)}$. ■

[STEP 2.2] For $i = 1, \cdots, m$, do the iteration (6). ■

[STEP 2.3] Let $\vec{\omega}^{(k+1)} = \vec{\omega}^{(k,m+1)}$. ■

[STEP 3] Suppose $\vec{\omega}^*$ is the final result of [STEP 2], then $\vec{x}^*$, whose j-th component is $x_j^* = |\omega_j^*|^{q-1} \mathrm{sign}(\omega_j^*)$, is the required result. ■

E. Dealing with Bound Constraint

In this subsection, we consider the bound-constrained minimum norm problem (PPB). This problem is equivalent to the following problem:

$$\text{minimize } F(\vec{x}) = \sum_{j=1}^{n} f(x_j) \text{ subject to } A\vec{x} = \vec{b}$$

where $f(t) = \begin{cases} t^p/p & 0 \le t \le 1 \\ \infty & \text{otherwise} \end{cases}$. The Lagrangian dual of the above problem is

$$\text{maximize } \vec{b}^\top \vec{y} - G(A^\top \vec{y})$$

where $G(\vec{x}) = \sum_{j=1}^{n} g(x_j),\ g(t) = \begin{cases} 0 & t < 0 \\ t^q/q & 0 \le t \le 1 \\ t - 1/p & t > 1 \end{cases}$. Similarly to the previous (PP) case, we can get the following iteration scheme which is like the iteration (6).

$$\omega_j^{(k,i+1)} = \omega_j^{(k,i)} + \beta a_{ij} \frac{b_i - \sum_{l=1}^{n} a_{il} g'(\omega_l^{(k,i)})}{\sum_{l=1}^{n} a_{il}^2 g''(\omega_l^{(k,i)})}.$$

Unfortunately, $g(t)$ does not have the second derivative at $t = 1$. Therefore, we define $g''(1) = q - 1$ for implementation. And we set the denominator of the fraction in the above iteration scheme to a real constant MIN if its value is less than MIN. Suppose $\vec{\omega}^*$ is the final result of the above iteration, then $\vec{x}^*$, whose j-th component is $x_j^* = g'(\omega_j^*)$, is the solution of the problem (PPB).

III. Experimental Results

A. Simulation Studies

We have applied the proposed method to reconstruct 3-D blood-vessel structure from a limited number of cone-beam projections. We have used the 3-D blood-vessel phantom developed by the phantom group of Siemens (http://www.imp.uni-erlangen.de/forbild/english/results/index.htm). The x-ray source positions are located on the circle with uniform angular interval over 180°. The number of source positions is 8 or 4 and each projection consists of 256×256 pixels. The reconstructed image has $256 \times 256 \times 256$ pixels. We have compared the proposed method with the conventional ART method which has been often used to this kind of limited-data problem in the literature. We used a projection data access order proposed in [4] which allows a fast convergence. By using this data access order, ten iterations were enough to obtain satisfactory images. The computations were performed with a PC with a Pentium III 700 MHz processer and the required computational time for ten iterations was about 30 minutes which is reasonable in practice. Five transaxial slices of reconstructed images after ten iterations are shown in Fig. 1 and Fig. 2 together with the corresponding slices of the phantom. In Fig. 3, we also show 3-D graphic display corresponding to the reconstructed images which is generated by using the volume rendering software. The threshold value to pick up the blood vessels from the reconstructed images is manually optimized dependent on each method. The proposed method succeeds in accurately reconstructing the fine blood-vessel structure whereas the ART method produces severe artifacts which make it impossible to recognize thin blood vessels. These results strongly demonstrate that the use of L_p norm with $p \approx 1.1$ is very powerful for sparse objects compared to $p = 2$ corrsponding to the ART method. Furthermore, the use of bound constraint $0 \le \vec{x} \le 1$ could improve the reconstructed images.

B. Real Data

We have also applied the proposed method to real data measured with our cone-beam tomographic imaging system using a synchrotron radiation x-ray source [5]. The cardiac blood-vessel phantom is used as a test object. The result will be presented at the conference. We are also applying the proposed method to cardiac SPECT data. The current result shows that the proposed method more accurately recovers the sharp boundary of blood pool compared with the ART method.

IV. Conclusions

We have proposed an accurate iterative method which is appropriate to reconstruct sparse objects from a limited number of projections. The main idea of the proposed method is to use the L_p norm with $p \approx 1.1$ to pick up a sparse solution from a set of feasible solutions. The algorithm is of row-action type and can be efficiently implemented similarly to the ART method. We have also shown that this method works well in the 3-D blood-vessel reconstruction from a limited number of cone-beam projections.

V. References

[1] D.Saint-Felix, Y.Trousset, C.Picard, C.Ponchut, R.Romeas, and A.Rougee," In vivo evaluation of a new system for 3D computerized angiography," Phys.Med.Biol., 39, pp.583-595, 1994

[2] D.P.Bertsekas," Non-linear programming," Athena Scientific, 1995

[3] Y.Censor and A.Lent," An iterative row-action method for interval convex programming," J.Opt.Theory Appl., 34, pp.321-353, 1981

[4] G.T.Herman and L.B.Meyer," Algebraic reconstruction techniques can be made computationally efficient," IEEE Trans.Med.Imaging, 12, pp.600-609, 1993

[5] T.Saito, H.Kudo, T.Takeda *et al.*," Three-dimensional monochromatic x-ray computed tomography using synchrotron radiation," Opt.Eng., 37, pp.2258-2268, 1998

[6] A.Dax," On minimum norm solutions," J.Opt.Theory Appl., 76, pp.183-193, 1993

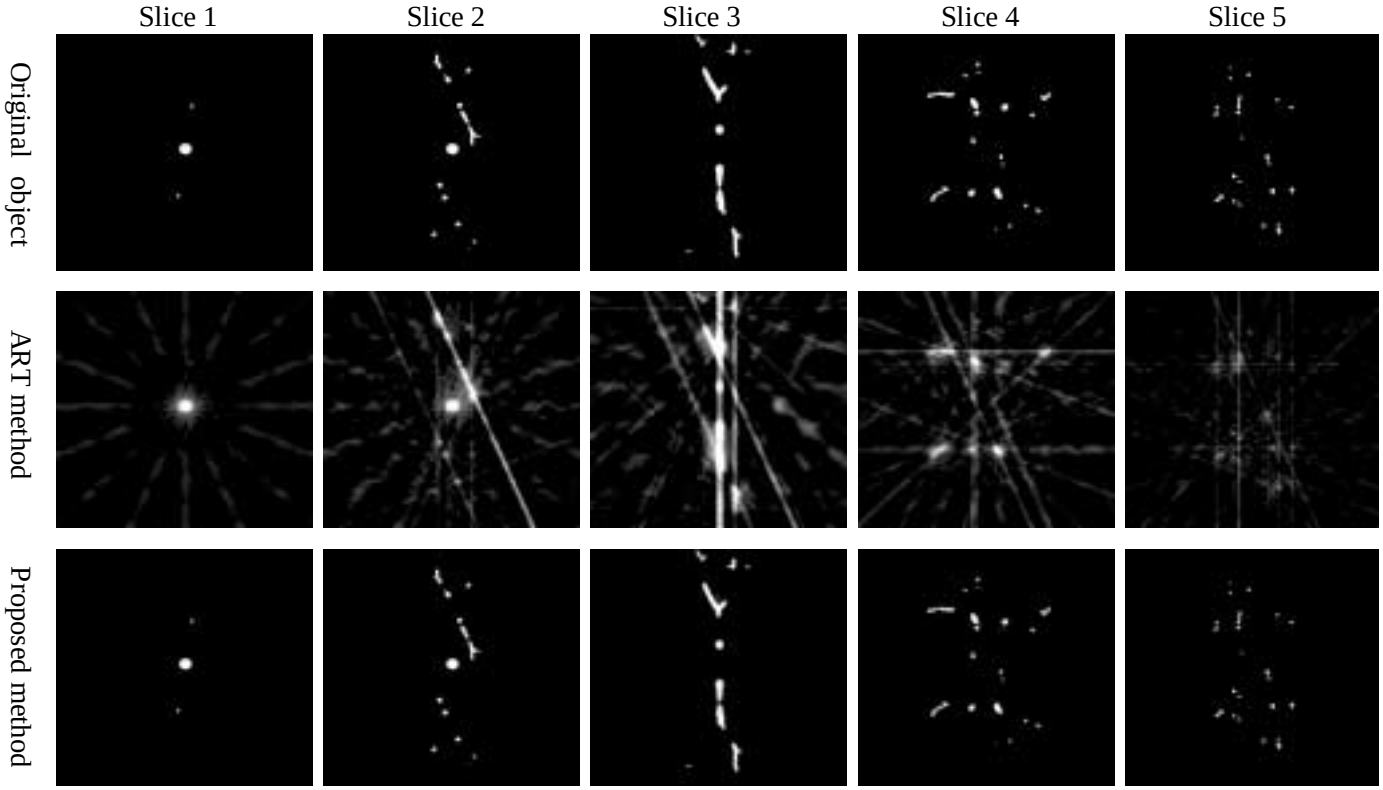

Fig. 1: Reconstructed transaxial slices from 8 projections.

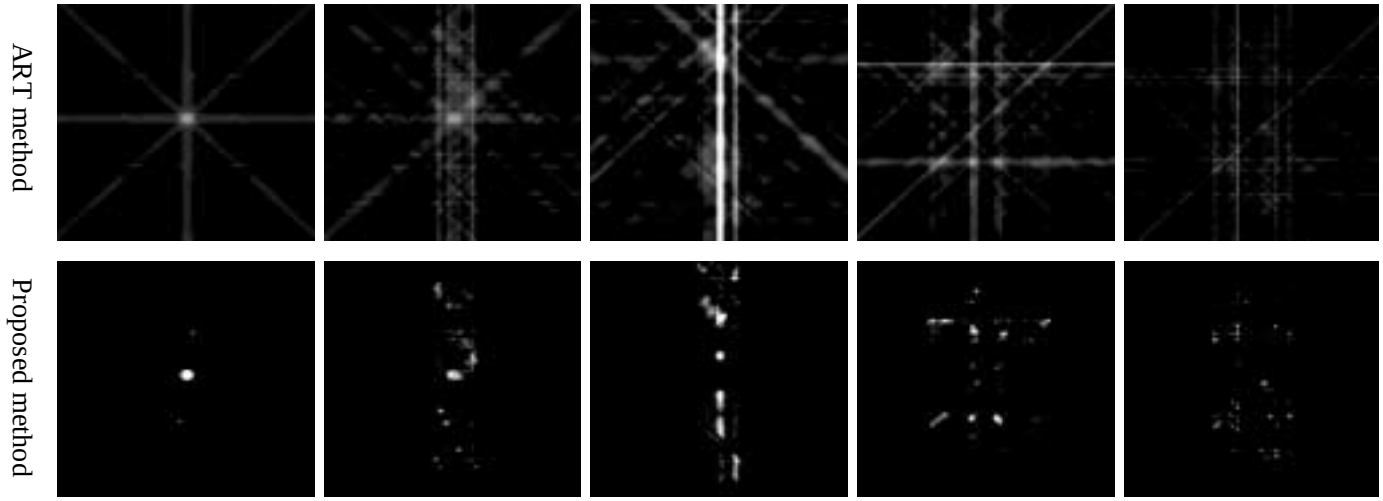

Fig. 2: Reconstructed transaxial slices from 4 projections.

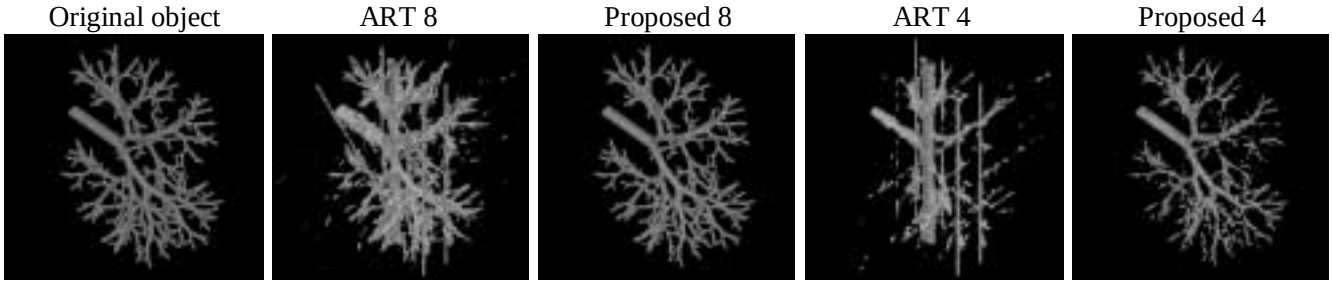

Fig. 3: 3-D graphic display of reconstructed images.